This is an *Accepted Manuscript*, which has been through the Royal Society of Chemistry peer review process and has been accepted for publication.

Accepted Manuscripts are published online shortly after acceptance, before technical editing, formatting and proof reading. Using this free service, authors can make their results available to the community, in citable form, before we publish the edited article. We will replace this *Accepted Manuscript* with the edited and formatted *Advance Article* as soon as it is available.

You can find more information about *Accepted Manuscripts* in the **Information for Authors**.

Please note that technical editing may introduce minor changes to the text and/or graphics, which may alter content. The journal's standard **Terms & Conditions** and the **Ethical guidelines** still apply. In no event shall the Royal Society of Chemistry be held responsible for any errors or omissions in this *Accepted Manuscript* or any consequences arising from the use of any information it contains.

Dalton Trans

ARTICLE TYPE

Spin-Orbit Effects in Square-Planar Pt(II) Complexes with Bidentate and Terdentate Ligands: Theoretical Absorption/Emission Spectroscopy

Christophe Gourlaouen,[a] **and Chantal Daniel**[a*]

The absorption and emission properties of a series of five Pt(II) planar complexes with bidentate ligands, namely [Pt(bpy)Cl$_2$] (bpy = 2,2'-bipyridine) **1** and [Pt(ppy)Cl$_2$]$^-$ (ppy = 2-phenylpyridine) **2** and terdentate ligands, namely [Pt(tpy)Cl]$^+$ (tpy = 2,2':6',2''-terpyridine) **3**, [Pt(phbpyR)Cl] (phbpy = 6-phenyl-2,2'-bipyridine; R = H) **4** and [Pt(dpybR)Cl] (dpyb = 2,6-di(2-pyridyl)benzene; R= CH$_3$) **5** have been investigated by means of density functional (DFT) and time-dependent DFT (TD-DFT) methods including solvent correction and 10 spin-orbit coupling (SOC). The DFT optimized structures of the five complexes in the electronic ground state agree with the experimental X-ray data and the theoretical absorption spectra reproduce quantitatively the main features of the experimental spectra. It is shown that the structures remain nearly planar in the low-lying singlet and triplet excited states of charge transfer character, metal-to-ligand (MLCT) or Cl to ligand (XLCT) whereas a significant distortion corresponding to the out-of-plane-bending of the Pt-Cl bond characterizes the geometry of the metal-centered (MC) states. In terdentate complexes **3**, **4** and **5** this distortion is energetically 15 unfavorable and not competitive with radiative decay via the low-lying MLCT and XLCT excited states. The absorption spectra of all complexes are significantly affected by spin-orbit coupling (red-shift and broadening), especially in the non-cyclometalated complexes **1** and **3** characterized by the presence of pure low-lying ^{3}MC states. The SOC effects are less important in the terpyridine complex **2** the lowest part of its spectrum being contaminated by mixed ^{3}MLCT/^{3}XLCT states. In the cyclometalated complexes **4** and **5** the presence of several LC states in the lowest part of the spectra is responsible for a small shift to the red as compared to the other complexes. The 20 solvatochromism that characterizes the absorption of this class of molecules in the visible is interpreted by the MLCT/XLCT mixed character of the excited states in this energy domain (400-450 nm). Indeed the solvent depedent XLCT contribution will control the magnitude of SOC in these excited states and will move the band to the red when diminishing and to the blue when increasing. As far as emission is concerned it is shown that strongly distorted non-radiative MC states minima, situated below the charge transfer states minima (ΔE = -0.3 eV to -0.8 eV) are easily accessible upon irradiation in the visible in complexes **1** and **3**, and in **2** to a lesser extend, 25 leading to no or low luminescence at room temperature. In contrast, the minima of the emissive states of mixed MLCT/XLCT/LC character are efficiently populated in **4** and **5**. The luminescence of complex **5**, cyclometalated in axial position, is particularly efficient because the minimum of the lowest emissive state is well separated from those of the MC states (ΔE = +0.23 eV) in contrast to its analog, complex **4**, cyclometalated in lateral position where the emissive MLCT/LC state minimum is nearly degenerate with the lowest MC state minimum (Δ = +0.01 eV).

30

[a] *Laboratoire de Chimie Quantique UMR-7177 CNRS-UdS, Université de Strasbourg, 1 Rue Blaise Pascal BP 296/R8 F-67008 Strasbourg, France.*

Tel. +33 03 88 6885 1314
e-mail addresss: c.daniel@unistra.fr

Dalton Transactions Accepted Manuscript

ARTICLE TYPE

Introduction

Luminescent square planar Pt(II) complexes coordinated to bidentate and terdentate ligands are of great interest in the development of new efficient organic light-emitting devices (OLED) or bio-imaging agents.[1,2,3] In third-row transition metal complexes fluorescence is not a concurrent process because of ultra-fast $S_n \rightarrow T_n$ intersystem crossing that populates the low-lying triplet excited states in a few picoseconds.[4,5,6] Consequently, the time-scale, quantum yield and wavelength of luminescence are entirely controlled by the character of the low-lying triplet states, namely metal-to-ligand-charge-transfer (MLCT), metal-centered (MC), ligand-centered (LC) or ligand-to-ligand-charge-transfer (LLCT). Hundred of new ligands have been synthesized in the past decades since the discovery of the first emissive Pt(II) complex [Pt(bpy)Cl$_2$] (bpy = 2,2'-bipyridine) **1** (SCHEME 1) and its derivatives.[7] The branching ratio between radiative and non-radiative decays is governed by ΔE, the energy gap between the lowest ^{3}MC state and the potentially emitting states, ^{3}MLCT or ^{3}LC, the coupling between the electronic ground states and the lowest triplet state and the medium (solution, solid). Whereas solid state may enhance luminescence intensity by formation of excimers accompanying a red shift of the emission,[8] strong coupling with the electronic ground state will favor non-radiative decay. Other parameters such as temperature effects may decrease quantum yield of luminescence by thermal activation of the non-radiative decay via the ^{3}MC state. In order to play with ^{3}MC/^{3}LC relative energies a number of complexes have been synthesized by substitution of Cl by other ligands such as cyano or thiolate groups leading to luminescent molecules in solution over a wide range of energies.[1] Unlike bidentate substituted complexes, flexible enough for efficient distortion of the N,N plan that stabilizes the ^{3}MC states, the more rigid terdentate family leads to efficiently luminescent molecules such as [Pt(tpy)Cl]$^+$ (tpy = 2,2':6',2''-terpyridine) **3** (SCHEME 1) under specific experimental conditions (in glassy solution).[9,10] The terdentate substituted complexes are characterized by a rich variety of emissive states, finely tune according to the structure and electronic properties of the ligands.[11]

The introduction of a covalent Pt-C bond in cyclometalated derivatives increases the ligand-field splitting by strong σ donation and destabilizes the MC states improving the emissive properties for efficient triplet emitters.[12,13,14,15,16] A small ΔE energy gap guarantees luminescence at low temperature only, as examplified by [Pt(ppy)Cl$_2$]$^-$ (ppy = 2-phenylpyridine) **2** (SCHEME 1).[17] A larger ^{3}MC/^{3}MLCT energy gap (> 3500 cm^{-1}) obtained by introducing a more rigid cyclometalated terdentate ligand that shortens the Pt-C bond and decreases the σ donation, leads to highly luminescent compounds. Combining small distortion in the excited state, Pt-C covalent bond, large ^{3}MC – ^{3}MLCT energy gap and weak coupling with the electronic ground states minimize non-radiative decay. This is illustrated by the terdentate [Pt(phbpyR)Cl] (phbpy = 6-phenyl-2,2'-bipyridine; R = H, CH$_3$) **4** and [Pt(dpybR)Cl] (dpyb = 2,6-di(2-pyridyl)benzene; R= H, CH$_3$) **5** complexes (SCHEME 1) that exhibit strong luminescence at room temperature in solution at 565 nm.[18,19] The position of the phenyl group may influence the emissive properties, especially the emission lifetime τ_{em} and quantum yield ϕ_{em} measured at 0.51 μs and 0.025 for **4** (phenyl in lateral position) and 7.2 μs and 0.6 for **5** (phenyl in central position). The colour is modulated by the auxiliary ligand R.[2,20,,21,22,23]

The huge experimental activity motivated by the search for new luminescent devices efficient over a wide range of energy and eventually applicable to bio-imaging,[24,25,26,27,28,29,30,31,32] is not balanced by substantial theoretical investigations. Most of the recent density functional theory (DFT) and time-dependent DFT (TD-DFT) based studies are dedicated to the interpretation of the puzzling experimental data and are devoted to structural and electronic properties of the ground state and lowest singlet S_1 and triplet T_1 excited states[25,26,28,33,34] sometimes supplemented by configuration interaction single (CIS) for the structural investigation of more S_n and T_n excited states.[35,36] Whereas the $S_0 \rightarrow S_n$ electronic absorption spectra are easily obtained by means of TD-DFT without or with solvent corrections, the emissive properties have been difficult to analyze until now because the determination of the degree of mixing between the singlet and triplet states by spin orbit coupling (SOC) and the systematic search for nuclear distortions in several close-lying excited states is still a challenge for computational chemistry. Tentative qualitative analysis based on Kasha rules for the determination of radiative vs. non-radiative decays rate constants from T_1 to S_0 has been applied with more or less success to square planar terdentate Pt(II) complexes.[37,38] An illustration is given in the recent paper by Che et al.[37] for some of the cyclometalated Pt(II) complexes discussed in the present article.

The recent improvement of quantum chemical methods for the exploration of electronic and geometrical structures of excited states including spin-orbit effects in transition metal complexes[39] extended the range of applications to semi-quantitative interpretation of absorption/emission spectroscopy in this class of molecules.[40,41,42,43,44,45,46,47,48]

Herein the electronic and geometrical structures of the ground state and lowest S_n and T_n excited states of bidentate complexes **1** and **2** and of terdentate complexes **3**, **4** and **5** depicted in SCHEME 1 and their absorption spectra are studied at the TD-DFT level, including solvent and SOC effects. Our goal is to compare and interpret the remarkable disparity in the emissive properties of these complexes, cyclometalated or not and representative of a wide class of square planar Pt(II) complexes investigated for their luminescent properties.
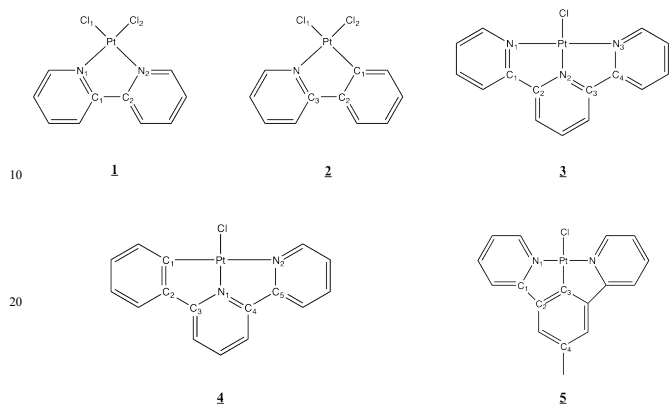
SCHEME 1. Schematic representation of [Pt(bpy)Cl$_2$] **1**, [Pt(ppy)Cl$_2$]$^-$ **2**, [Pt(tpy)Cl]$^+$ **3**, [Pt(phbpyH)Cl] **4** and [Pt(dpybR)Cl] **5** (R = CH$_3$).

Computational details

The electronic ground states geometries of the five complexes **1**-**5** depicted in SCHEME 1 have been optimized by means of density functional theory (DFT) with the B3LYP functional[49,50] without any symmetry constraint for **1**-**4** and in Cs symmetry for **5**, using the all-electrons scheme and a triple-ζ polarized basis set (TZP).[51] The scalar relativistic effects have been introduced by the zeroth order regular approximation ZORA,[52] the spin-orbit corrections being included as a perturbation. The nature of the stationary state was checked through a complete set of real frequencies.

The transition energies to the low-lying singlet and triplet excited states have been computed by means of time-dependent DFT (TD-DFT) method[53,54] including solvent corrections for dichloromethane (ε = 8.9, rad =2.94 Å) through the Conductor like screening model (COSMO)[55,56,57] as implemented in ADF[58,59]. The geometries of the low-lying singlet and triplet states have been optimized at the TD-DFT level using a state specific approach. In case of low-lying triplet metal-centered ^{3}MC excited states geometry optimization by means of TD-DFT may fail because of near-degeneracy problems. In these cases (complexes **1**, **3** and **4**) the optimized structures have been obtained by Δ-SCF procedure. The B3LYP results have been validated by the TD-DFT computation of the theoretical absorption spectrum of complex **2** [Pt(ppy)Cl$_2$]$^-$ by means of CAM-B3LYP functional developed for long-range charge transfer states.[60] The computation of the emissive properties, namely the optimization of the lowest triplet and singlet excited states potential energy minima, has been performed without spin-orbit perturbation. The absorption and emissive properties of complex **2** [Pt(ppy)Cl$_2$]$^-$ have been computed within the Tamm-Dancoff Approximation (TDA)[61] as well in order to check a possible over stabilization of the lowest LC states. The analysis of the theoretical absorption spectra is based on electron density differences computed from Kohn-Sham orbitals and their occupations in the electronic ground state and excited states using the DGRID package from Kohout.[62] The composition of the "spin-orbit" states En is determined by the percentage of the singlet Sn and triplet Tn "spin-free" components generated by SOC. The shape of the theoretical spectra has been constructed by Gaussian fit (fwhm = 15). The B3LYP, CAM-

B3LYP and TDA theoretical absorption spectra of complex [Pt(ppy)Cl$_2$]$^-$ **2** are represented in Figures S1 and S2 (SI section).

The calculations have been performed with ADF quantum chemistry software.[63]

Results

Structure and absorption spectroscopy of polypyridine complexes [Pt(bpy)Cl$_2$ **1** and [Pt(tpy)Cl]$^+$ **3**

Some important optimized bond lengths and bond angles of complexes **1** and **3** are reported in Table 1 for the electronic ground state and some of the lowest excited states. X-ray data are provided, when available for comparison.[64,65]

-Table 1-

Table 1. Some important DFT/B3LYP optimized bond lengths (in Å) and bond angles (in °) of [Pt(bpy)Cl$_2$] **1** and [Pt(tpy)Cl]$^+$ **3** in the electronic ground state S$_0$ and lowest singlet S$_n$ and triplet T$_n$ excited states (numbering of the atoms according to SCHEME 1). The states are labeled according to their adiabatic transition energies given in eV.

The absorption spectroscopy of complexes **1** and **3** is composed essentially of ligand-centered (LC), MC, MLCT and XLCT excited states. SCHEME 2 represents the electronic densities characterizing important excited states reported in Table 2, selected for their contribution to the theoretical absorption spectra of [Pt(bpy)Cl$_2$] **1** and [Pt(tpy)Cl]$^+$ **3**, respectively.
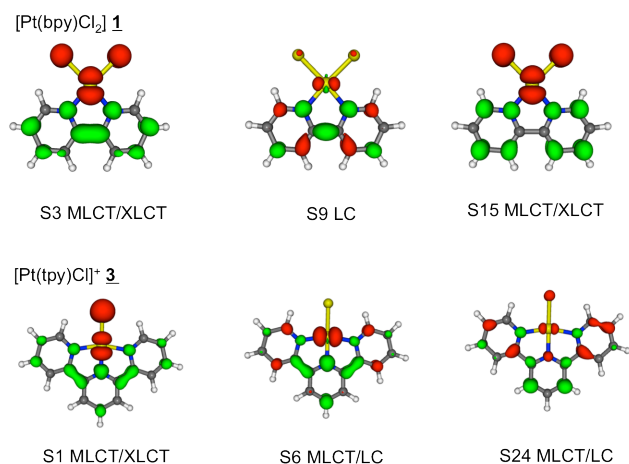
SCHEME 2. Electronic densities characterizing important excited states reported in Table 2, selected for their contribution to the theoretical absorption spectra of [Pt(bpy)Cl$_2$] **1** and [Pt(tpy)Cl]$^+$ **3** (Color code; red: decrease in density, green: increase in density).

When relaxing the geometries the character of the excited states as well as their relative energies are modified, eventhough the main electronic composition is usually preserved. In the bipyridine complex **1** the MLCT and XLCT states or their mixed counterpart MLCT/XLCT or XLCT/MLCT, remain nearly planar with a geometry very similar to the electronic ground state S$_0$. The

agreement between the theoretical structures in the electronic ground state and the experimental structures is rather good in both complexes **1** and **3**. The S_1, T_2 and T_3 excited states of **3**, corresponding to MLCT, MLCT/LC and LC/MLCT/XLCT states are nearly planar. In contrast the MC states, namely T_1 and T_2 in [Pt(bpy)Cl$_2$] **1** and T_1 in [Pt(tpy)Cl]$^+$ **3** are strongly distorted with a significant opening of the Cl-Pt-N bond angle and an out-of-plane bending of the Pt-Cl bond (Table 1) leading to a non-planar conformation. The population and stabilization of these low-lying ^{3}MC states will be highly effective only when this strong distortion will be facilitated by experimental conditions, namely temperature, flexible ligand or counterion influence. From this point of view, the theoretical results clearly confirm the experimental observations.

The energetics of the optimized excited states defined by the adiabatic transition energies in Table 1, will be discussed in the section devoted to emission properties.

The vertical TD-DFT/B3LYP transition energies to the low-lying singlet excited states of [Pt(bpy)Cl$_2$] **1** and [Pt(tpy)Cl]$^+$ **3** with significant oscillator strengths (f > 0.075) are reported in Table 2 and the corresponding absorption spectra are represented in Figures 1 and 2, respectively. The vertical transition energies to the full set of singlet and triplet states can be found in the SI section (Table S1).

The absorption spectra of **1** and **3** including SOC are represented in Figures 1 and 2 (in red), respectively whereas the energetics of the low-lying excited states calculated with SOC is given in Table 3.
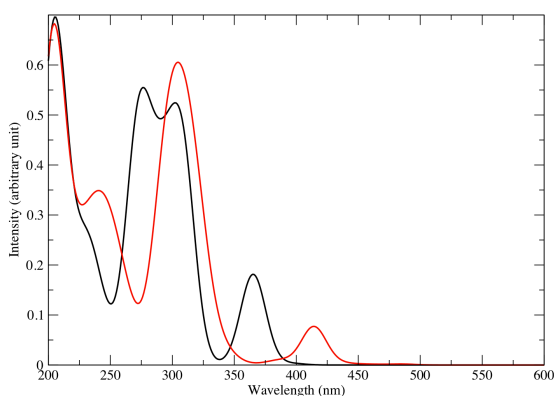
Figure 1. Theoretical (TD-DFT/B3LYP) absorption spectrum of [Pt(bpy)Cl$_2$] **1** without (in black) and with SOC (in red).

The theoretical absorption spectrum of [Pt(bpy)Cl$_2$] **1** is dominated by MLCT/XLCT transitions and characterized by one first intense band centered at 365 nm (without SOC, Table 2) shifted to 418 nm when SOC is included (E16, Table 3). This red shift is accompanied by a large SO mixing between S3 (43%) and T7 (42%) leading to the MLCT/XLCT maximum at 418 nm, the electronic density of which is represented in SCHEME 2. The upper MLCT/XLCT states compose the next intense band characterized by a double peak with maxima at 308 nm (S9) and 292 nm (S11) (without SOC). The band at 308 nm corresponds mainly to a LC transition. When SOC is activated these two bands mix to give E42 and E50 and merge into a single peak centered at 310 nm. The upper band calculated at 204 nm with a weak shoulder at 230 nm is assigned to MLCT/LC and XLCT transitions. Whereas the maximum at 205 nm is not affected by SOC and remains purely singlet LC (E157), the MLCT/XLCT states are reorganized by SO mixing leading to a more intense shoulder at ~250 nm composed of XLCT transitions (E92, E96, Table3). Low-lying excited states of weak oscillator strengths (f < 10^{-2}) generated by spin-orbit splitting of the lowest ^{3}MC (T3, T4, Table 3) compose the lowest experimental absorption starting at 475 nm whatever the solvent is (di-chloromethane or butyronitrile).[66] The experimental absorption spectrum of [Pt(bpy)Cl$_2$] **1** is also characterized by an intense band extremely solvent dependent, observed at 345 nm in water, 415 nm in chlorobenzene, 394 nm in butyronitrile. This solvent dependent absorption can be attributed to the first intense MLCT/XLCT band at 365 nm (418 nm with SOC). Indeed, the XLCT contribution to this band will vary as function of the solvent polarity. Since the SOC effect increases with the MLCT (or MC) character it will be indirectly solvent dependent and produces a more or less significant solvatochromism. The experimental features correlate rather well with the SOC/TD-DFT absorption spectrum of [Pt(bpy)Cl$_2$] **1** represented in Figure 1.

-Table 2-

Table 2. TD-DFT/B3LYP transition energies (in eV) to the low-lying singlet excited states of [Pt(bpy)Cl$_2$] **1** and [Pt(tpy)Cl]$^+$ **3**, absorption wavelengths (in nm) and associated oscillator strengths f (> 0.075).

The theoretical absorption spectrum [Pt(tpy)Cl]$^+$ **3** represented in Figure 2 exhibits two intense peaks at 250 nm and 326 nm corresponding to LC/MLCT and MLCT/LC mixed states, respectively (Table 2). When SOC is included the band at 320 nm, predominantly MLCT, is red shifted and splitted into several shoulders whereas the LC/MLCT peak at 250 nm remains but decreases in intensity. The band covering the region between 370 nm and 383 nm is red shifted by SOC to 390 - 445 nm (Table 3) and is assigned to mixed MLCT/XLCT and MC states of weak oscillator strengths. The shape of the theoretical absorption spectrum of **3** calculated with SOC (Figure 2) agrees rather well with the experimental one (inset in Figure 2) recorded in acetonitrile[67] and with most recent data in methanol.[68] In contrast to [Pt(bpy)Cl$_2$] **1**, that was characterized by a lowest MC state calculated at 488 nm (Table 3), the lowest part of the spectrum of the terpyridine complex **3** shows three low-lying MLCT/XLCT states, the first MC states being calculated at 410 nm and 402 nm (Table 3). This difference leading to a more important red-shift of the lowest absorption band in **1** than in **3** can only be obeserved when spin-orbit is included.
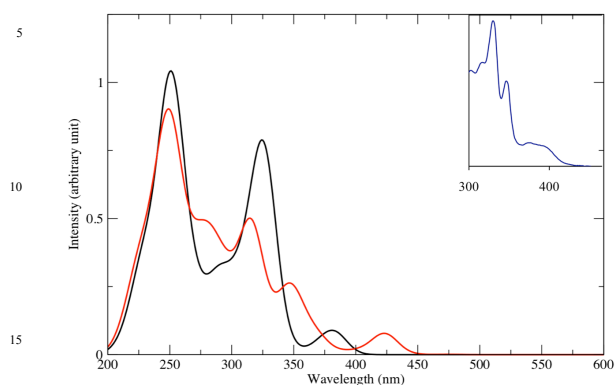
Figure 2. Theoretical (TD-DFT/B3LYP) absorption spectrum of [Pt(tpy)Cl]$^+$ **3** without (in black) and with SOC (in red); the experimental spectrum is represented in the inset (by courtesy of Dr. D. R. McMillin).

-Table 3-

Table 3. Vertical TD-DFT/B3LYP transition energies (in eV) including SOC to the low-lying E_n excited states of [Pt(bpy)Cl$_2$] **1** and [Pt(tpy)Cl]$^+$ **3**, corresponding absorption wavelengths (in nm) and associated oscillator strengths (f>0.001 below 370 nm and f>0.05 above 375 nm).

Structure and absorption spectroscopy of cyclometalated complexes [Pt(ppy)Cl$_2$]$^-$ 2, [Pt(phbpyH)Cl] 4 and [Pt(dpybR)Cl] 5 (R = CH$_3$)

Some important optimized bond lengths and bond angles of complexes **2**, **4** and **5** are reported in Table 4 for the electronic ground state and lowest excited states. X-ray data are provided, when available for comparison.[69,70,71]

-Table 4-

Table 4. Some important DFT/B3LYP optimized bond lengths (in Å) and bond angles (in °) of [Pt(ppy)Cl$_2$]$^-$ **2**, [Pt(phbpyR)Cl] **4** and [Pt(dpybR)Cl] **5** (R = CH$_3$) (C$_s$ symmetry) in the electronic ground state S$_0$ and lowest singlet and triplet excited states (Numbering of the atoms according to SCHEME 1). The excited states are labeled according to their adiabatic transition energies given in eV.

SCHEME 3 represents the electronic densities characterizing important excited states reported in Table 5, selected for their contribution to the theoretical absorption spectra of [Pt(ppy)Cl$_2$]$^-$ **2**, [Pt(phbpyH)Cl] **4** and [Pt(dpybR)Cl] **5** (R = CH$_3$). Whatever the functional used, B3LYP or CAM-B3LYP the excited states of **2** are very similar in nature. Only the B3LYP results are discussed here.
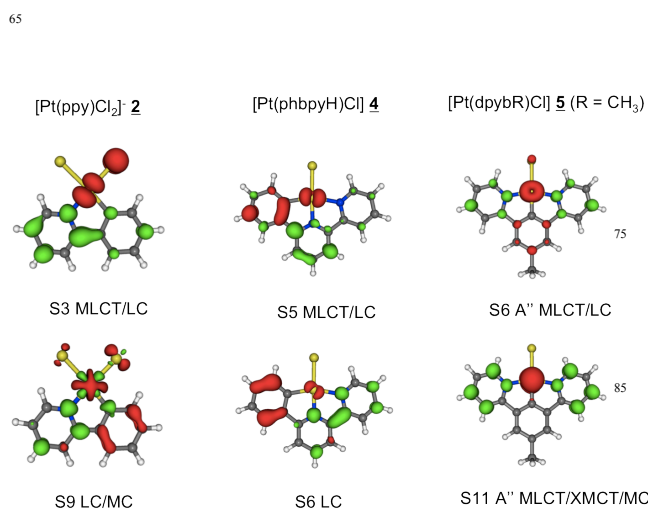
SCHEME 3. Electronic densities characterizing important excited states reported in Table 5, selected for their contribution to the theoretical absorption spectra of [Pt(ppy)Cl$_2$]$^-$ **2**, [Pt(phbpyH)Cl] **4** and [Pt(dpybR)Cl] **5** (R = CH$_3$) (Color code; red: decrease in density, green: increase in density).

The theoretical geometries of the three complexes, **2**, **4** and **5**, in the electronic ground states agree with the experimental structures as illsutrated by the values reported in Table 4. In general the cyclometalated complexes are less distorted in the excited states than the bipyridine and terpyridine complexes **1** and **3** discussed in the previous section. In [Pt(ppy)Cl$_2$]$^-$ **2** the major deformations correspond to significant elongation of the Pt-Cl and Pt-N bonds whatever the nature of the excited state, MC, MLCT or of mixed charge-transfer character, keeping a nearly planar structure. In contrast, the lowest MC states of [Pt(phbpyH)Cl] **4** and [Pt(dpybR)Cl] **5** (R = CH$_3$) are characterized by an out-of-plane deformation, especially critical in the T$_3$ and T$_4$ MC states of the strongly emissive complex **5** and to a lesser extend in the T$_2$ MC state of **4**. The optimized geometries of the two low-lying nearly degenerate T$_3$ and T$_4$ MC states in **5** are represented in SCHEME 4. Whereas in T$_4$ the deformation corresponds to a "classical" out-of-plane bending of the Pt-Cl bond, in T$_3$ the metal atom Pt is out-of-plane as well.

[Pt(dpybR)Cl] R=CH$_3$
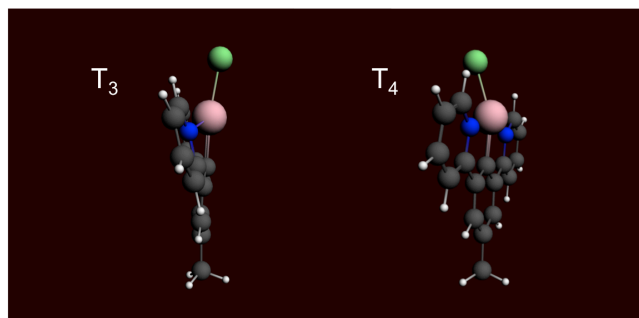
SCHEME 4. Optimized geometries of the two low-lying nearly degenerate T_3 and T_4 MC states in [Pt(dpybR)Cl] (R = CH$_3$) **5** (Table 4).

The vertical TD-DFT/B3LYP transition energies to the low-lying singlet excited states of [Pt(ppy)Cl$_2$]$^-$ **2**, [Pt(phbpyH)Cl] **4** and [Pt(dpybR)Cl] **5** (R = CH$_3$) are reported in Table 5 and the corresponding absorption spectra are represented in Figures 3,4 and 5, respectively. The vertical transition energies to the full set of singlet and triplet states can be found in Table S2 in the SI section. The absorption spectra of **2, 4** and **5** including SOC are represented in Figure 3, 4 and 5 (in red), respectively whereas the energetics of the low-lying excited states calculated with SOC is given in Table 6.

The theoretical absorption spectrum of [Pt(ppy)Cl$_2$]$^-$ **2** including SOC starts at ~ 470 nm in agreement with the experimental spectra of this specific complex and of other cyclometalated related molecules.[72,73] The broadening and extension to the red by SOC effect of the two lowest bands calculated at 396 nm (S1) and 346 nm (S3) (Table 5 and Figure 3, black) is due to a large SO mixing between S1 / S3 and a number of low-lying MLCT/XLCT and MC triplet states, among them T3, T6 and T7 (Table 6). This results into a broad band calculated between 473 nm (E1, Table 6) and 375 nm (E18, Table 6) corresponding to the slightly solvatochromic absorption observed between 365 nm and 400 nm.[72] Similarly to [Pt(bpy)Cl$_2$] **1** the solvatochromism comes from the XLCT contributions that may vary as function of the solvent polarity influencing the SOC effects. The overall shape of the theoretical spectrum characterized by a second absorption region starting at 330 nm with a maximum at 300 nm followed by a peak at 250 nm and a very intense absorption at 212 nm agrees rather well with the experimental spectra of phenylpyridine substituted complexes recorded in solution.[73] Whereas the first band at 300 nm composed of S9, S10 and S12 states is not affected by SOC effects, the peak at 250 nm (S18, S21) is red shifted to 265 nm by some triplet contribution (Table 6). The SOC effects on the theoretical absorption spectrum of the simplest cyclometalated complex [Pt(ppy)Cl$_2$]$^-$ **2** are less significant than in the bipyridine complex [Pt(bpy)Cl$_2$] **1**. This is due to minor contributions of MC states in the lowest region of the absorption spectrum of **2**.

-Table 5-

Table 5. TD-DFT/B3LYP transition energies (in eV) to the low-lying singlet excited states of [Pt(ppy)Cl$_2$]$^-$ **2**, [Pt(phbpyH)Cl] **4** and [Pt(dpybR)Cl] **5** (R = CH$_3$), absorption wavelengths (in nm) and associated oscillator strengths (f > 0.035).
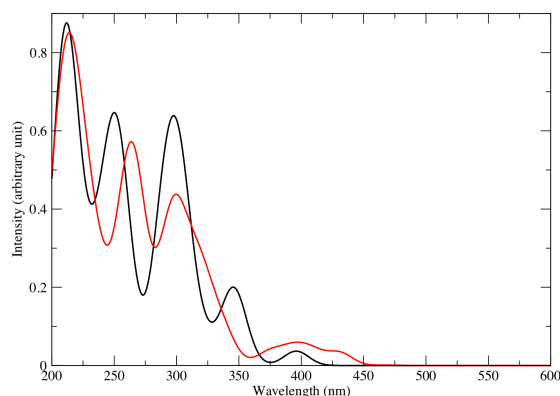
Figure 3. Theoretical (TD-DFT/B3LYP) absorption spectrum of [Pt(ppy)Cl$_2$]$^-$ **2** without (in black) and with SOC (in red).

The theoretical TD-DFT/B3LYP absorption spectra of [Pt(ppy)Cl$_2$]$^-$ **2** represented in Figure 3 can be compared to the TD-DFT/CAM-B3LYP and TD-DFT/TDA depicted in Figures S1 and S2 (SI section). The lowest part of the theoretical absorption spectrum is blue-shifted by 40-50 nm when using CAM-B3LYP. This shift is a little bit more important in the upper part of the spectrum because of the presence of pure IL states in the UV and far UV domain of energy. The spectra calculated within the TDA, including or not SOC (Figure S2, SI section), are very similar to the TD-DFT/B3LYP absorption spectra (Figure 3).

The theoretical absorption spectrum of [Pt(phbpyH)Cl] **4**, cyclometalated in lateral position, starts at 520 nm when SOC is included (Table 6, Figure 4, in red) in agreement with the experimental spectrum recorded in dichloromethane that shows an absorption tail between 450 nm and 500 nm.[74] This part of the spectrum is assigned to SOC splitted ^{3}MLCT and ^{3}MLCT/XLCT states (E1 to E5, Table 6) of very weak oscillator strengths (<10^{-3}). The solvatochromic band observed between 400 nm and 445 nm corresponds to the MLCT/XLCT transition calculated at 455 nm (Table 6, Figure 4, in red). The two intense peaks with calculated maxima at 343 nm and 294 nm (without SOC, Table 5) correspond to LC states and the third one at 235 nm is assigned to a MLCT state. When including SOC these three peaks lose in intensity by mixing with a number of MLCT/XLCT states generating a broad absorption between 400 nm and 220 nm with several more or less intense peaks (Figure 4, in red). The LC states (Tabel 5, S6, S11) are slightly affected by SOC leading to two nearly pure states E36 and E68 of same transition energies (Table 6) in contrast to the upper MLCT state (Table 5, S30). The low-lying ^{3}MC states contributions occur beyond 370 nm and do not perturb the lowest part of the theoretical absorption spectrum. The theoretical spectrum reproduces the overall experimental shape of the experimental spectrum of [Pt(phbpyH)Cl] **4** characterized by three peaks at 330 nm, 275 nm and 220 nm.[74]
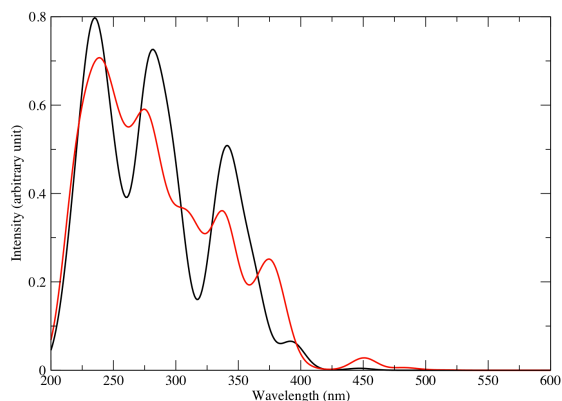
Figure 4. Theoretical (TD-DFT/B3LYP) absorption spectrum of [Pt(phbpyH)Cl] **4** without (in black) and with SOC (in red).
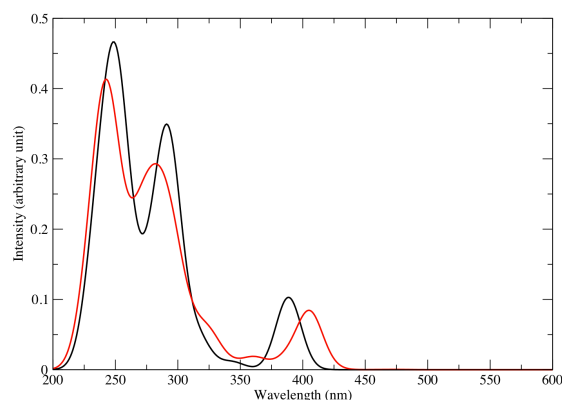
Figure 5. Theoretical (TD-DFT/B3LYP) absorption spectrum of [Pt(dpybR)Cl] **5** (R = CH$_3$) without (in black) and with SOC (in red).

The theoretical absorption spectrum of [Pt(dpybR)Cl] **5** (R = CH$_3$), cyclometalated in axial position, begins at 480 nm when SOC is taking into account with two MLCT transitions of weak intensities (Table 6) followed by a first LC/XLCT/MLCT state calculated at 408 nm and remaining purely singlet after SOC treatment (E7). A moderate red-shift of the lowest band is observed in this complex mainly governed by singlet/triplet SO mixing of the lowest LC/MLCT states. Similarly to [Pt(phbpyH)Cl] **4** there is no significant ^{3}MC contribution below 262 nm. Consequently the shapes of the theoretical spectra calculated without SOC (Figure 5, black) and with SOC (Figure 5, red) are very similar with two bands of increasing intensities, the first one covering the 303 nm-271 nm region, the second one centered at 247 nm (E59, Table 6). Two shoulders are present at 366 nm and 330 nm as observed in the experimental spectrum (380 nm, 332 nm) recorded in CH$_2$Cl$_2$.[19] The lowest part of the experimental spectrum is characterized by three bands at 401 nm, 454 nm and 485 nm attributed to the LC/XLCT/MLCT transition (408 nm) and to the lowest states (E1, E2) generated by SOC splitting of the two lowest ^{3}MLCT states and calculated at 465 nm and 480 nm (Table 6).

-Table 6-

Emission spectroscopy of polypyridine complexes [Pt(bpy)Cl$_2$ 1 and [Pt(tpy)Cl]$^+$ 3

The TD-DFT/B3LYP adiabatic and vertical T$_n$ → S$_0$ transition energies and corresponding emission wavelengths of [Pt(bpy)Cl$_2$ **1** and [Pt(tpy)Cl]$^+$ **3** are reported in Table 7.

-Table 7-

Table 7. TD-DFT/B3LYP adiabatic and vertical T$_n$ → S$_0$ transition energies (in eV) and corresponding emission wavelengths (in nm) of [Pt(bpy)Cl$_2$ **1** and [Pt(tpy)Cl]$^+$ **3**. The states are ordered and labeled according to their adiabatic transition energies as in Table 1.

The emissive properties of complexes [Pt(bpy)Cl$_2$ **1** and [Pt(tpy)Cl]$^+$ **3** are governed by the presence of two low-lying MC states, the minima of which are calculated at 1.49 eV and 2.21 eV, respectively, well below the potentially emissive minima. These MC states are easily accessible after visible irradiation and stabilized by the out-of-plane deformation that characterizes these T$_1$ states (Table 1). A highly probable coupling with the electronic ground state is responsible for the quenching of emission in these two molecules at room temperature. In the terdentate complex **3** the proximity of an emissive state T$_2$ of MLCT/LC character calculated at 2.54 eV (Table 7) and emitting at 645 nm explains the observed luminescence under specific experimental conditions.[9,10]

Emission spectroscopy of cyclometallated complexes [Pt(ppy)Cl$_2$]$^-$ 2, [Pt(phbpyR)Cl] 4 and [Pt(dpybR)Cl] 5 (R = CH$_3$)

The TD-DFT/B3LYP adiabatic and vertical T$_n$ → S$_0$ transition energies and corresponding emission wavelengths of [Pt(ppy)Cl$_2$]$^-$ **2**, [Pt(phbpyH)Cl] **4** and [Pt(dpybR)Cl] **5** (R = CH$_3$) are reported in Table 8. The vertical T$_n$ → S$_0$ transition energies calculated within the TDA for [Pt(ppy)Cl$_2$]$^-$ **2** are given in parenthesis for comparison. In contrast to recent studies reported for Ir[75] and Ru[76] complexes, both methods provide very similar emissive properties in terms of state character and transition energies for this complex validating the B3LYP results discussed in this section.

-Table 8-

Table 8. TD-DFT/B3LYP adiabatic and vertical T$_n$ → S$_0$ transition energies (in eV) and corresponding emission wavelengths (in nm) [Pt(ppy)Cl$_2$]$^-$ **2**, [Pt(phbpyH)Cl] **4** and [Pt(dpybR)Cl] **5** (R = CH$_3$). The states are ordered and labeled according to their adiabatic transition energies as in Table 4.

Whereas [Pt(ppy)Cl$_2$]$^-$ **2** and [Pt(phbpyH)Cl] **4** should be trapped

into the lowest T_1 MLCT/XLCT/LC and MLCT/LC states, respectively calculated at 2.49 eV in **2** and 2.30 eV in **4**, for developping emissive properties, complex **5**, cyclometalated in axial position, is characterized by two states T_1 and T_2 of MLCT/LC/XLCT character, calculated at 2.52 eV and 2.58 eV and emissive at 513 nm and 500 nm, respectively.

In **4**, cyclometalated in lateral position, the proximity of one MC state calculated at 2.31 eV (T_2) and nearly degenerate with the T_1 emissive state calculated at 2.30 eV (Table 8) is probably responsible for the low observed quantum yield of emission of this complex at room temperature.[18] Moreover the structural deformation needed for stabilizing the T_2 state in **4** is not very important (Table 4) and this MC state should be easily populated.

In complex **5**, characterized by a very efficient emission at about 565 nm,[19] the MC states T_3 and T_4, the electronic densities of which are represented in SCHEME 5, are well above the emissive states (about + 0.25 eV) and need strong distortion of the complex to be efficiently populated and stabilized as illustrated by their optimized geometries depicted in SCHEME 4 and discussed in the previous section.

[Pt(dpybR)Cl] R=CH$_3$

T$_4$ (A') ^{3}MC   T$_3$ (A'') ^{3}MC
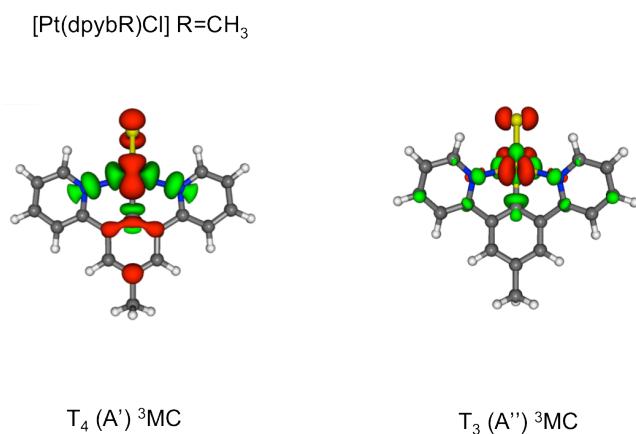
SCHEME 5. Electronic densities characterizing the MC excited states T_3 and T_4 of [Pt(dpybR)Cl] **5** (R = CH$_3$) (Table 8) (Color code; red: decrease in density, green: increase in density).

The cyclometalated terdentate complex [Pt(phbpyR)Cl] **4** is the only complex where one singlet state (S_1) calculated at 2.55 eV and of MLCT/LC character, is competitive with the low-lying triplet for participating to the emission of this molecule at an estimated wavelength of 527 nm (Table 8). In the other complexes the optimized minima of the singlet states are well above those of the triplet states and cannot participate to the obseved luminescence.

The estimated wavelengths of emission reported in Tables 7 and 8 for complexes **1**, **3**, **2**, **4** and **5** do not take into account the SOC, namely the splitting of the lowest states and their mixing with singlet states. Indeed the determination of optimized structures in electronic excited states including SOC is simply impossible in transition metal complexes with the nowdays computational methods. Moreover, as illustrated by the "spin-orbit" states reported in Tables 3 and 6 and calculated at the geometry of the S_0

electronic ground state, the triplet states splitting and the contamination by singlet contributions is generally insignificant in the lowest states.

Conclusion

Five square planar Pt(II) complexes with bidentate and terdentate ligands, cyclometalated or not, and representative of a large number of molecules synthesized for their luminescent properties over a wide range of energy have been investigated by means of DFT and TD-DFT approaches.

The theoretical absorption spectra computed with SOC and solvent corrections reproduce the main experimental features and point to the presence of low-lying triplet states (MC, MLCT/XLCT) participating to the absorption between 450 nm and 500 nm. SOC effects have to be included to obtain realistic spectra quantitatively similar to the experimental spectra. The complexes are characterized by low-lying states of mixed character including charge transfer from the metal or the halide to the π^* acceptor ligands as well as LC components entirely localized on the bidentate and terdentate ligands.

The MC states are strongly distorted as compared to the charge transfer or ligand localized excited states, especially in the non-cyclometalated complexes. The MC states are stabilized by important out-of-plane deformations accompanied by the bending of the Pt-Cl bond whereas the other excited states remain nearly planar.

The emissive properties of the series of complexes have been rationalized on the basis of the optimized structures and energetics of the low-lying singlet and triplet excited states. The presence of low-lying MC states easily populated upon visible irradiation and stabilized by out-of-plane distortion explains the poor luminescence of the bipyridine and terpyridine non-cyclometalated complexes at room temperature. In contrast, the cyclometalated molecules possess low-lying emissive MLCT/LC excited states easily populated, especially in the terdentate complexes. The presence of these states associated to MC states situated well above, needing strong structural stabilizing out-of-plane deformation for being populated optimise the effectiveness of luminescence in these complexes.

The usual oversimplified picture of one single T_1 triplet state responsible for the luminescent properties of the Pt square planar complexes discussed above is far from being realistic. The presence of several close low minima opening the route to spin-orbit/vibronic couplings induced decays via potential wells of excited states of various natures renders luminescence process into a very complicated mechanism not easily detectable by standard spectroscopies. Modern computational theory may tackle the challenge of interpreting and rationalizing this intricate photophysics characterized by fluctuating radiative decay rates and luminescence efficiencies. These observables are entirely controlled by subtle changed of electronic densities coupled to small structural distortions themselves correlated to the metal/ligand/substituants/media/temperature interplay.

national IDRIS (Paris) and CINES (Montpellier) computer centres through a grant of computer time by GENCI, and at the regional HPC centre (Strasbourg).

References

1 J. A. G. Williams, *Top. Curr. Chem.*, 2007, **281**, 205 and references therein.

2 J. A. G. Williams, *Chem. Soc. Rev.*, 2009, **38**, 1783 and references therein.

3 L. Murphy, J. A. G. Williams, *Top. Organomet. Chem.*, 2010, **28**, 75 and references therein.

4 A. Cannizzo, A. M. Blanco-Rodríguez, A. El Nahhas, J. Sebera, S. Zális, A. Vlček Jr., M. Chergui, *J. Am. Chem. Soc.*, 2008, **130**, 8967-8974.

5 G. J. Hedley, A. Ruseckas, I. D. W. Samuel, *J. Phys. Chem. A,*2009, **113**, 2.

6 Ch. Bressler, C. Milne, V.-T. Pham, A. El Nahas, R. M. van der Veen, W. Gawelda, S. Johnson, P. Beaud, D. Grolimund, M. Kaiser, C. N. Borca, G. Ingold, R. Abela, M. Chergui, M. *Science*, 2009, **323**, 489.

7 V. M. Miskowski, V. H. Houlding, *Inorg. Chem.*, 1989, **28**, 1529; V. M. Miskowski, V. H. Houlding, C. –M. Che, Y. Wang, *Inorg. Chem.*, 1993, **32**, 2518.

8 W. B. Connick, L. M. Henling, R. E. Marsh, H. B. gray, *Inorg. Chem.*, 1996, **35**, 6261.

9 J. A. Bailey, M. G. Hill, R. E. Marsh, V. M. Miskowski, W. P. Schaefer, H. B. gray, *Inorg. Chem.,* 1995, **34**, 4591.

10 J. F. Michalec, S. A. bejune, D. G. Cuttell, G. C. Summerton, J. A. Gertenbach, J. S. Field, J.S. Haines, D. R. McMillin, *Inorg. Chem.* 2001, **40**, 2193.

11 D. K. C. Tears, D. R. McMillin, *Coord. Chem. Rev.*, 2001, **211**, 195; D. R. McMillin, J. J. Moore, *Coord. Chem. Rev.*, 2002, **229**, 113.

12 L. Chassot, E. Müller, A. von Zelewsky, *Inorg. Chem.*, 1984, **23**, 4249.

13 M. Maestri, D. Sandrini, V. Balzani, L. Chassot, P. jolliet, A. von Zelewsky, *Chem. Phys. Lett.*, 1985, **122**, 375.

14 F. Barigelletti, D. Sandrini, M.Maestri, V. Balzani, A. von Zelewsky, L. Chassot, P. Jolliet, U. Maeder, *Inorg. Chem.*, 1988, **27**, 3644.

15 H. Yersin, D. Donges, *Top. Curr. Chem.*, 2001, **214**, 81.

16 R. C. Evans, P. Douglas, C. J. Winscom, *Coord. Chem. Rev.*, 2006, **250**, 2093.

17 P. –I. Kvam, M. V. Puzyk, K. P. Balashev, J. Songstad, *Acta Chem. Scand.*, 1995, **49**, 335.

18 T. –C. Cheung, K. –K. Cheung, S. –M. Peng, C. –M. Che, *J. Chem. Soc. Dalton Trans*, 1990, 1645.

19 J. A. G. Williams, A. Beeby, E. S. Davies, J. A. Weinstein, C. Wilson, *Inorg. Chem.*, 2003, **42**, 8609.

20 S. –W. Lai, M. C. –W. Chan, T. –C. Cheung, S. –M. peng, C. –M. Che, *Inorg. Chem.*, 1999, **38**, 4046.

21 S. C. F. Kui, I. H. T. Sham, C. C. C. Cheung, C. –W. Ma, B. Yan, N. Zhu, C. –M. Che, *Chem. Commun.* 2002, 900.

22 K. –H. Wong, M. C. -W. Chan, C. –M. Che, *Chem. Eur. J.*, 1999, **5**, 2845.

23 C. –M. Che, W. –F. Fu, S. –W. Lai, Y. –J. Hou, Y. –L. Liu, *Chem. Commun.*, 2003, 118.

24 W. Lu, B. –X. Mi, M. C. W. Chan, Z. Hui, C. –M. Che, N. Zhu, S. –T. Lee, *J. Am. Chem. Soc.*, 2004, **126**, 4958.

25 H. Guo, S. Ji, W. Wu, W. Wu, J. Shao, J. Zhao, *Analyst*, 2010, **135**, 2832.

26 K. –W. Wang, J. –L. Chen, Y. –M. Cheng, M. –W. Chung, C. –C. Hsieh, G. –H. Lee, P. –T. Chou, K. Chen, Y. Chi, *Inorg. Chem.*, 2010, **49**, 1372.

27 I. Stengel, C. A. Strassert, E. A. Plummer, C. –H. Chien, L. De Cola, P. Bäuerle, *Eur. J. Inorg. Chem.*, 2012, 1795.

28 E. S. –H. Lam, D. P. –K. Tsang, W. H. lam, A. Y. –Y. Tam, M. –Y. Chan, W. –T. Wong, V. W. –W. Yam, *Chem. Eur. J.* 2013, **19**, 6385.

29 S. Y. –L. Leung, E. S. –H. Lam, W. H. Lam, K. M. –C. Wong, W. –T. Wong, V. W. –W. Yam, *Chem. Eur. J.*, 2013, **19**, 10360.

30 M. Cocchi, J. Kalinowski, D. Virgili, V. Fattori, S. Develay, J. A. G. Williams, *Appl. Phys. Lett.*, 2007, **90**, 163508.

31 S. J. Farley, D. L. Rochester, A. L. Thompson, J. A. K. Howard, J. A. G. Williams, *Inorg. Chem.*, 2005, **44**, 9690.

32 J. Brooks, Y. Babayan, S. Lamansky, P. I. Djurovich, I. Tsyba, *Inorg. Chem.*, 2002, **41**, 3055.

33 X. –Y. Hu, X. –J. Liu, J. –K. Feng, *Chin. J. Chem.,* 2007, **25**, 1370.

34 Y. Zhang, J. A. Garg, C. Michelin, T. Fox, O. Blacque, K. Venkatesan, *Inorg. Chem.*, 2011, **50**, 1220.

35 X. Zhou, H. –X. Zhang, Q. –J. Pan, B. –H. Xia, A. –C. Tang, *J. Phys. Chem. A.*, 2005, **109**, 8809.

36 X. –J. Liu, J. –K. Feng, J. Meng, Q. –J. Pan, A. –M. Ren, X. Zhou, H. –X. Zhang, *Eur. J. Inorg. Chem.* 2005, 1856.

37 G. S. –M. Tong, C. –M. Che, *Chem. Eur. J.*, 2009, **15**, 7225.

38 W. H. Lam, E. S. –H. lam, V. W. –W. yam, *J. Am. Chem. Soc.*, 2013, **135**, 15135.

39 C. Daniel, *Coord. Chem. Rev.* In press 2014.

40 X. Li, B. Minaev, H. Ångren, H. Tian, Eur. J. *Inorg. Chem.*, 2011, 2517.

41 R. Bakova, M. Chergui, C. Daniel, A. Vlcek Jr, S. Zalis, *Coord. Chem. Rev.,* 2011*,* **255**, 975.

42 H. Brahim, C. Daniel, A. Rahmouni, *Int. J. Quant. Chem.*, 2012, **112**, 2085.

43 R. Heydova, E. gindensperger, R. Romano, J. Sykora, A. Vlcek Jr, S. Zalis, C. Daniel, *J. Phys. Chem. A*, 2012,**116**, 11319.

44 H. Brahim, C. Daniel *Comp. Theor. Chem.* 2014, in press, http://dx.doi.org/10.1016/j.comptc.2014.01.030.

45 E. Jansson, B. Minaev, S. Schrader, H. Ågren, *Chem. Phys.*, 2007, **333**, 157.

46 X. Li, B. Minaev, H. Ågren, H. tian, J. Phys. Chem. C, 2011, 115, 20724.

47 S. Zális, C. J. Milne, A. E. Nahhas, A. M. Blanco-Rodriguez, R. M. van der Veen, A. Vlcek Jr, *Inorg. Chem.*, 2013, **52**, 5775.

48 C. Sousa, C. de Graaf, A. Rudavskyi, R. Broer, J. Tatchen, M. Etinski, C. M. Marian, *Chem. Eur. J.,* 2013, **19**, 17541.

49 A. D. Becke, *J. Chem. Phys,.* 1993, **98**, 5648.

50 P. J. Stephens, F. J. Devlin, C. F. Chabalowski, M. J. Frisch, *J. Phys. Chem.,* 1994, **98**, 11623.

51 E. van Lenthe, E. J. Baerends, *J. Comp. Chem.* 2003, **24**, 1142.

52 E. van Lenth, R. van Leeuwen, E. J. Baerends, J. G. Snijders, *Int. J. Quant. Chem.* 1996, **57**, 281.

53 E. Runge, E. K. U. Gross, E. K. U., Phys. Rev. Lett. 52 (12) (1984) 997.

54 M. Petersilka, U. J. Gossmann, E.K.U. Gross, *Phys. Rev. Lett.* 76 (8) (1996) 1212.

55 A. Klamt, G. Schüürmann, *J. of Chem. Soc.: Perkin Trans.*, 1993, **2**, 799.

56 A. Klamt, *J. Phys. Chem.,* 1995, 99, 2224.

57 A. Klamt, V. Jones, *J. Chem. Phys.*, 1996, **105**, 9972.

58 A. Rosa, E. J. Baerends, S. J. A. van Gisbergen, E. van Lenthe, J.A. Groeneveld, J. G. Snijders, *J. Am. Chem. Soc.* 1999, **121**, 10356.

59 C. C. Pye, T. Ziegler, *Theo. Chem. Acc.,* 1999, **101**, 396.

60 T. Yanai, D. P. Tew, N. C. Handy, *Chem. Phys. Lett.*, 2004, **343**, 51.

61 M. J. Peach, D. J. Tozer, *J. Phys. Chem. A*, 2012, **116**, 9783.

62 M. Kohout, DGrid, version 4.5, Radebeul, **2009**.

63 ADF2013, SCM, Theoretical Chemistry, Vrije Universiteit, Amsterdam, The Netherlands: https://www.scm.com/Downloads/2013)

64 R. H. Herber, M. Croft, M. J.Coyer, B. Bilash, A. Sahiner, *Inorg. Chem.*, 1994, **33**, 2422.

65 R. Zhang, Z. Liang, A. Han, H. Wu, P. Du, W. Lai, R. Cao, *Cryst. Eng. Comm.*, 2014, doi:10.1039/C4CE00514G.

66 V. M. Miskowski, V. H. Houlding, Inorg. Chem., 1989, 28, 1529.

67 T. K. Aldridge, E. M. Stacy, D. R. McMillin, Inorg. Chem., 1994, **33**, 722.

68 G. Arena, G. Calogero, S. Campagna, L. M. Scolaro, V. Ricevuto,† and R. Romeo, *Inorg. Chem.,* 1998, *37,* 2763-2769.

69 P. I. Kvam, T. Engebretsen, K. Maartmann-Moe, J. Songstad, *Acta Chem. Scandinavica*, 1996, **50**, 107.

70 Y. Kataoka, Y. Kitagawa, T. Kawakami, M. Okumura *J. Organom. Chem.*, 2013, *743*, 163.

71 A. Hofmann, L. Dahlenburg, R. van Eldik, *Inorg. Chem.* 2003, **42**, 6528.

72 P. –I. Kvam, M. V. Puzyk, K. P. Balashev, J. Songstad, *Acta Chem. Scand.*, 1995, **49**, 335.

73 J. Brooks, Y. Babayan, S. Lamansky, P. I. Djurovich, I. Tsyba, R. bau, M. E. Thompson, *Inorg. Chem.*, 2002, **41**, 3055.

74 T. -C. Cheung, K. –K. Cheung, S. –M. Peng, C. –M. Che, *J. Chem. Soc. Dalton Trans.*, 1996, 1645.

75 R. M. Edkins, K. Fucke, M. J. G. Peach, A. G. Crawford, T. B. Marder, A. Beeby, *Inorg. Chem.*, 2013, **52**, 9842.

76 T. Very, D. Ambrosek, M. Otsuka, C. Gourlaouen, X. Assfeld, A. Monari, C. Daniel, Chem. A Eur. J. Manuscript Number: chem.201402963R2, accepted June 2014.

Theoretical "Spin-free" (in black) and "Spin-orbit" (in red) absorption spectra of $[Pt(tpy)Cl]^+$ and electronic densities characterizing the main intense bands MLCT/XLCT at 384 nm, MLCT/LC at 326 nm and 250 nm (experimental spectrum in inset).